

# 1 **Vitreous fluid-isolated DNA for the genetic analysis of** 2 **primary uveal melanoma: a proof-of-concept study**

## 3 **Authors**

4 R.J. Nell<sup>1</sup>

5 M. Versluis<sup>1</sup>

6 N.V. Menger<sup>1</sup>

7 M.C. Gelmi<sup>1</sup>

8 T.H.K. Vu<sup>1</sup>

9 R.M. Verdijk<sup>2,3</sup>

10 G.P.M. Luyten<sup>1</sup>

11 M.J. Jager<sup>1</sup>

12 P.A. van der Velden<sup>1\*</sup>

13

14 <sup>1</sup> Department of Ophthalmology, Leiden University Medical Center, Leiden, the Netherlands.

15 <sup>2</sup> Department of Pathology, Leiden University Medical Center, Leiden, the Netherlands.

16 <sup>3</sup> Department of Pathology, Section Ophthalmic Pathology, Erasmus MC University Medical  
17 Center, Rotterdam, the Netherlands.

18

19 \* Corresponding author, Department of Ophthalmology, Leiden University Medical Center,  
20 PO Box 9600, 2300 RC Leiden, The Netherlands.

21

## 22 **Acknowledgements**

23 This study was supported by the European Union's Horizon 2020 research and innovation  
24 program under grant agreement number 667787 (UM Cure 2020, R.J. Nell and N.V.  
25 Menger). The authors thank the UM Cure 2020 consortium partners and patient  
26 organisations for their helpful discussions regarding this research project.

## 27 **Abstract**

### 28 **Background**

29 Uveal melanoma is an aggressive ocular malignancy. Early molecular characterisation of  
30 primary tumours is crucial to identify those at risk of metastatic dissemination. Although  
31 tumour biopsies are being taken, liquid biopsies of ocular fluids may form a less invasive but  
32 relatively unexplored alternative. In this study, we aim to evaluate the DNA content of  
33 vitreous fluid from eyes with a uveal melanoma to obtain molecular information from the  
34 tumour.

35

### 36 **Methods**

37 DNA was isolated from 65 vitreous fluid samples from enucleated eyes with a uveal  
38 melanoma and studied using digital PCR. Primary and additional driver mutations (in *GNAQ*,  
39 *GNA11*, *PLCB4*, *CYSLTR2*, *BAP1*, *SF3B1* and *EIF1AX*) were investigated using accustomed  
40 targeted and drop-off assays. The copy numbers of chromosome 3p and 8q were measured  
41 using multiplex and single-nucleotide polymorphism-based assays. Our findings were  
42 compared to the molecular profile of matched primary tumours and to the clinicopathological  
43 tumour characteristics.

44

### 45 **Results**

46 Almost all (63/65) vitreous fluids had measurable levels of DNA, but melanoma-cell derived  
47 DNA (containing the primary driver mutation) was detected in 39/65 samples (median  
48 proportion 18%, range 0.2%-94%) and was associated with a larger tumour prominence, but  
49 not with any of the molecular tumour subtypes. Among the vitreous fluids with melanoma-cell  
50 derived DNA, not all samples harboured (analysable) other mutations or had sufficient  
51 statistical power to measure copy numbers. Still, additional mutations in *BAP1*, *SF3B1* and  
52 *EIF1AX* were detected in 13/15 samples and chromosome 3p and 8q copy numbers  
53 matched the primary tumour in 19/21 and 18/20 samples, respectively. Collectively, a  
54 clinically-relevant molecular classification of the primary tumour could be inferred from 27/65  
55 vitreous fluids.

56

### 57 **Discussion**

58 This proof-of-concept study shows that substantial amounts of DNA could be detected in  
59 vitreous fluids from uveal melanoma patients, including melanoma-cell derived DNA in 60%  
60 of the samples. Prognostically-relevant genetic alterations of the primary tumour could be  
61 identified in 42% of the patients. A follow-up study is needed to evaluate our approach in a  
62 prospective clinical context.

## 63 Introduction

64 Uveal melanoma is a rare, aggressive intraocular tumour originating from malignantly-  
65 transformed melanocytes in the iris, ciliary body or choroid (**Figure 1**). The majority of uveal  
66 melanomas are located in the relatively inconspicuous and inaccessible posterior segment of  
67 the eye [1]. Consequently, primary tumours can be large upon first detection and  
68 (micro)metastases may occur before first treatment [2, 3]. For that reason, early and  
69 adequate identification and characterisation of primary uveal melanomas is crucial to prevent  
70 tumour progression and ameliorate patient outcome.

71  
72 Over the past decades, prognostically-relevant molecular tumour subtypes have been  
73 identified based on the genetic alterations present in the primary uveal melanoma. Tumours  
74 with *EIF1AX* mutations are generally copy number stable and have the best prognosis with  
75 the lowest risk of early metastatic dissemination [4, 5]. *SF3B1*-mutant tumours often present  
76 with additional copies of chromosome 8q and are associated with an intermediate prognosis  
77 with relatively late metastases [4, 6-8]. Uveal melanomas with a loss of chromosome 3p and  
78 a *BAP1* mutation, typically also showing chromosome 8q copy number increases, have the  
79 poorest prognosis [9, 10].

80  
81 Primary uveal melanoma is usually treated by local, eye-preserving procedures  
82 (brachytherapy, proton beam therapy) or a complete surgical removal of the eye  
83 (enucleation) [1]. In case of the latter, tumour tissue is readily available for molecular  
84 analysis, and such analysis is usually offered to all enucleated patients. For non-enucleated  
85 patients, however, an additional tumour biopsy is required to obtain a molecular profile of the  
86 melanoma. While intra-ocular fine-needle aspirate tumour biopsies are being taken routinely  
87 in a number of clinics, the procedure is relatively invasive and remains accompanied by  
88 various risks [11, 12]. A less invasive (outpatient) biopsy procedure would allow more  
89 patients to have a personalised molecular diagnosis and prognosis. Moreover, those with an  
90 increased risk of metastatic dissemination may be offered a more intense follow-up  
91 screening program, and could possibly benefit from earlier detection of metastasis.  
92 Additionally, knowledge about the molecular profile of the primary tumour has been positively  
93 associated with various aspects of psychosocial well-being [13] and might be of (future)  
94 clinical relevance with regard to novel (neo-)adjuvant therapies [5, 14, 15].

95  
96 Previously, we introduced digital PCR assays to analyse the key genetic alterations in uveal  
97 melanoma to quantify the intratumour heterogeneity in bulk tumour specimens [16-20].  
98 Digital PCR can also be used for the sensitive detection of genetic alterations in scarce DNA

99 samples, such as liquid biopsies (i.e. samples of body fluids such as blood or serum, urine or  
100 aspirates) [21]. In this study (**Figure 1**), we isolate DNA from 65 vitreous fluid samples  
101 obtained from enucleated eyes with a uveal melanoma. These samples are analysed for  
102 mutations in *GNAQ*, *GNA11*, *PLCB4*, *CYSLTR2*, *EIF1AX*, *SF3B1* and *BAP1*, and copy  
103 number alterations (CNAs) affecting chromosomes 3p and 8q. Next, our findings are  
104 compared to the molecular profile of matched primary tumours and to the clinicopathological  
105 tumour characteristics. Collectively, this study forms the proof-of-concept for a  
106 comprehensive characterisation of the DNA content of the vitreous as a potential liquid  
107 biopsy for uveal melanoma patients to identify those at high risk of developing metastases.

## 108 **Materials and methods**

### 109 **Vitreous fluid sample collection and DNA isolation**

110 Vitreous fluid samples were collected from 65 enucleated eyes with a uveal melanoma as  
111 part of the biobank of the Department of Ophthalmology, Leiden University Medical Center  
112 (LUMC). Samples had been isolated by syringe suction directly after opening the enucleated  
113 eye, and stored at -80 °C. This study was approved by the LUMC Biobank Committee and  
114 Medisch Ethische Toetsingscommissie under numbers B14.003/SH/sh and B20.026/KB/kb.

115  
116 Total DNA was isolated from 100-200 uL vitreous fluid, using the Quick-cfDNA Serum &  
117 Plasma Kit (Zymo Research, Irvine, USA) and eluted in 35 uL DNA elution buffer (Zymo),  
118 following the manufacturer's instructions. From all samples, the matched primary uveal  
119 melanoma was analysed in our recent study using digital PCR and targeted DNA and RNA  
120 sequencing [20]. Clinical and molecular information of all samples is summarised in

121 **Supplementary Table 1.**

122

### 123 **Digital PCR experiments**

124 All digital PCR experiments were carried out using the QX200 Droplet Digital PCR System  
125 (Bio-Rad Laboratories, Hercules, USA) using the assays and following the protocols  
126 described earlier [16-20, 22]. Typically, 3.5 uL isolated vfdNA was analysed in a single 22 uL  
127 experiment, using 11 uL ddPCR™ Supermix for Probes (No dUTP, Bio-Rad) and primers  
128 and FAM- or HEX-labelled probes in final concentrations of 900 and 250 nM for duplex  
129 experiments, or optimised concentrations for multiplex experiments. Assay details are  
130 described in our recent study [20].

131

132 All PCR mixtures were partitioned into 20,000 droplets using the AutoDG System (Bio-Rad).  
133 Next, a PCR protocol was performed in a T100 Thermal Cycler (Bio-Rad): 10 minutes at 95  
134 °C; 30 seconds at 94 °C and 1 minute at 55 °C, 58 °C or 60 °C for 40 cycles; 10 minutes at  
135 98 °C; cooling at 12 °C for up to 48 hours, until droplet reading. Ramp rate was set to 2  
136 °C/second for all steps.

137

138 Reading of the droplets was performed using the QX200 Droplet Reader (Bio-Rad). The raw  
139 results of the digital PCR experiments were acquired using *QuantaSoft* (version 1.7.4, Bio-  
140 Rad) and imported and analysed in the online digital PCR management and analysis  
141 application *Roodcom WebAnalysis* (version 2.0, available via  
142 <https://webanalysis.roodcom.nl>).

143

144 First of all, the  $G\alpha_q$  signalling mutations (in *GNAQ*, *GNA11*, *CYSLTR2* and *PLCB4*) were  
145 analysed in duplex experiments and the measured concentrations (listed between square  
146 brackets) of the mutant and wild-type alleles were used to calculate the total vfdNA  
147 concentrations and melanoma-cell derived vfdNA fractions:

148

$$149 \quad \text{total vfdNA concentration} = [\text{mutation}] + [\text{wildtype}]$$

150

$$151 \quad \text{melanoma-cell derived vfdNA fraction} = 2 \cdot \frac{[\text{mutation}]}{[\text{mutation}] + [\text{wildtype}]}$$

152

153 Additional BSE mutations in *BAP1*, *SF3B1* and *EIF1AX* were interpreted in a qualitative  
154 manner only.

155

156 CNAs were measured via two different approaches [19]. Following the classic approach,  
157 copy number values were calculated based on the measured concentrations of a DNA target  
158 on chromosome 3p (*PPARG*) and 8q (*PTK2*), and a reference gene on chromosome 5p  
159 (*TERT*) or 14q (*TTC5*) assumed to be stable:

160

$$161 \quad \text{copy number value} = 2 \cdot \frac{[\text{target}]}{[\text{reference}]}$$

162

163 Following the SNP-based approach, copy number values were measured using the  
164 concentrations of haploid genomic loci  $\text{var}_1$  and  $\text{var}_2$ , representing the two variants of a  
165 heterozygous SNP:

166

$$167 \quad \text{copy number value} = 1 + \frac{[\text{var}_1]}{[\text{var}_2]}$$

168

169 In this formula, the SNP variant in the denominator ( $\text{var}_2$ ) is the one that was assumed to be  
170 unaltered and copy number stable (i.e. haploid). Analysed SNPs in this study included  
171 rs6617, rs6976, rs9586, rs1989839, rs1062633 and rs2236947 on chromosome 3p, and  
172 rs7018178 and rs7843014 on chromosome 8q.

173

#### 174 **In silico evaluation of digital PCR sensitivity and power prediction**

175 To evaluate the statistical power of detecting CNAs in the vfdNA+/UM+ samples, we  
176 performed *in silico* digital PCR simulations using our R library *digitalPCRsims*

177 (available via <https://github.com/rjnell/digitalPCRsimulations>), as described recently [19]. In  
178 short, for each individual sample, we determined the sensitivity (% of simulated experiments)  
179 of detecting a chromosomal loss (copy number = 1) or gain (copy number = 3), assuming  
180 that this alteration is clonally present in the entire vfDNA melanoma-cell population. An  
181 alteration was considered 'detected' when the obtained copy number was lower or higher  
182 than 2 and the constructed 99%-confidence interval did not contain 2. The input vfDNA  
183 concentration and melanoma-cell fraction were based on the initial  $G\alpha_q$  mutation and wild-  
184 type measurements. The total amount of accepted droplets was set to 15,000 and each  
185 condition was simulated up to 1,000 times. An experimental setup (classic or SNP-based  
186 approach) was considered 'underpowered' in samples with a sensitivity <80% when  
187 analysing a maximum of 45,000 droplets.

188

### 189 **Statistical analysis and code availability**

190 Statistical evaluations in this study were conducted using Spearman's rank correlation  
191 coefficient, Fisher's exact test, the Mann-Whitney  $U$  test and the log-rank test. All analyses  
192 were performed using R version 4.0.3 in RStudio version 1.4.1103. All custom scripts are via  
193 <https://github.com/rjnell/um-vitreous>.

## 194 Results

### 195 DNA composition of vitreous fluid samples assessed by mutant and wild-type Gα<sub>q</sub>

196 Gα<sub>q</sub> signalling mutations at established hotspots in *GNAQ*, *GNA11*, *CYSLTR2* and *PLCB4*  
197 are considered the initiating events driving the development of uveal melanoma [18, 23-28].  
198 As they form the most clonal and most common genetic alteration in the primary tumour, they  
199 represent a relatively generic marker of the malignant cells that can be used to quantify the  
200 abundance of melanoma-cell derived DNA [20]. Based on the exact Gα<sub>q</sub> mutation that was  
201 identified earlier in the matched primary tumour [20], we investigated all vitreous fluid DNA  
202 (vfDNA) samples using targeted digital PCR for the absolute and relative abundance of  
203 mutant and wild-type DNA (**Figure 2 and 3A**).

204  
205 We did not find mutant or wild-type alleles in 2/65 (3%) samples, indicating that these  
206 samples did not contain measurable amounts of vfDNA (**Figure 2**). Wild-type Gα<sub>q</sub> alleles only  
207 were detected in 24/65 (37%) vitreous fluid samples; these samples were labelled as  
208 vfDNA+/UM-, as they had measurable levels of vfDNA but lacked DNA that was derived  
209 from mutant melanoma cells (**Figure 2 and 3A**). Still, they contained up to ~1500 genomic  
210 copies per uL vitreous fluid (median 22 genomic copies per uL). In one vfDNA+/UM- patient,  
211 the primary uveal melanoma was known to carry two clonally-abundant Gα<sub>q</sub> signalling  
212 mutations (*GNA11* p.R183H and *PLCB4* p.D630N in vfDNA-29), but the vfDNA only  
213 contained wild-type *GNA11* and *PLCB4* in comparable concentrations.

214  
215 Mutant Gα<sub>q</sub> alleles were detected in 39/65 (60%) samples, which were labelled as  
216 vfDNA+/UM+ (**Figure 2 and 3A**). In these samples, the sum of mutant and wild-type allele  
217 concentrations was taken as total vfDNA concentration (median 134 genomic copies per uL).  
218 The mutant allele fractions were used to estimate the abundance of melanoma-cell derived  
219 vfDNA, revealing proportions between 0.2% and 94% (median 18%). vfDNA+/UM+ samples  
220 also contained significantly more non-melanoma cell derived vfDNA (i.e. DNA not derived  
221 from uveal melanoma cells, Mann-Whitney U  $p = 0.011$ ) than vfDNA+/UM- samples (**Figure**  
222 **3B**).

223

### 224 Analysis of additional BSE mutations in *BAP1*, *SF3B1* and *EIF1AX*

225 Besides the generic Gα<sub>q</sub> mutations, the majority of all uveal melanomas are known to carry  
226 an additional 'BSE mutation' in *BAP1*, *SF3B1* or *EIF1AX* [4, 7, 9]. In contrast to the Gα<sub>q</sub>  
227 mutations, however, only a subset of those BSE mutations can be found at a hotspot  
228 position. In our cohort of primary uveal melanomas from vfDNA+/UM+ patients [20], *BAP1*

229 alterations occurred throughout the entire gene, most of the *SF3B1* mutations affected  
230 position p.R625, and *EIF1AX* mutations were found at various positions within the first two  
231 exons of the gene (**Supplementary Table 1**).

232  
233 To be able to analyse these diverse BSE mutations, we developed a variety of targeted and  
234 generic drop-off digital PCR assays [20]. Hereby, a small number of unique *BAP1* alterations,  
235 all hotspot mutations in *SF3B1* (p.R625C/H), and all mutations in *EIF1AX* (exon 1 and exon  
236 2) could be analysed (**Figure 4 and Supplementary Table 1**). We now applied these assays  
237 in the corresponding cohort of vfDNA+/UM+ samples (n=15). A selection of vfDNA+/UM-  
238 samples with matched total vfDNA concentrations were measured as negative controls  
239 (**Figure 4**). Based on the known mutational status of the respective primary tumours, *EIF1AX*  
240 mutations were successfully identified in 5/6 vitreous fluid samples, *SF3B1* mutations in 5/6  
241 samples and *BAP1* mutations in 5/5 samples (**Figure 2**). Two samples (vfDNA-07 and  
242 vfDNA-56) carried two BSE mutations, which were both detected in the vfDNA. Of note, the  
243 two vitreous fluid samples with undetected BSE mutations (vfDNA-23 and vfDNA-49) had  
244 two of the lowest concentrations of Gα<sub>q</sub> mutant alleles within the vfDNA+/UM+ cohort (**Figure**  
245 **2 and Supplementary Table 1**). In total, 13/15 (87%) of the analysed vitreous fluid samples  
246 had a measurable BSE mutation matching with the corresponding primary tumour.

247

#### 248 **Advanced chromosome 3p and 8q copy number analysis**

249 CNAs are usually studied by comparing the absolute abundance of a target of interest to a  
250 stable genomic reference (classic approach, **Figure 5A**) [19]. As an alternative, CNAs may  
251 be measured by evaluating the allelic (im)balance between the two variants of a  
252 heterozygous SNP on the chromosome of interest (SNP-based approach, **Figure 5A**). While  
253 both SNP variants are equally abundant under healthy conditions, this balance is altered  
254 when there is a copy number loss or gain of one of the alleles. Conveniently, a stable  
255 genomic reference is not required when using this approach and more precise  
256 measurements can be obtained. We recently validated this methodology for detecting  
257 chromosome 3p and 8q alterations in uveal melanoma [19].

258

259 The precision of digital PCR measurements also depends on the amount of DNA input  
260 (limited by the low quantity of our samples) and the number of partitions (i.e. droplets) [19]. A  
261 typical digital PCR experiment yields between 10,000 and 20,000 droplets, but this can be  
262 increased by repeating the experiment and merging the results into one combined analysis.  
263 The limiting factor, however, remains that those experimental replicates also require more  
264 sample DNA. To determine the statistical power of both the classic and SNP-based approach

265 in our application of analysing samples with diverse total and melanoma-cell derived vfDNA  
266 concentrations, we performed *in silico* simulations based on the initial G $\alpha$ <sub>q</sub> mutant and wild-  
267 type measurements of all vfDNA+/UM+ samples. For each individual sample, we evaluated  
268 the sensitivity of detecting a chromosomal loss (copy number = 1) or gain (copy number = 3)  
269 assuming that this alteration is clonally present in the vfDNA melanoma-cell population. As  
270 representative examples, the *in silico* analyses and *in vitro* observations for measuring  
271 chromosome 3p loss in samples vfDNA-41 and vfDNA-24 are presented in **Figure 5B and C**.  
272 A summary of the analyses for all samples is given in **Supplementary Table 1**.

273  
274 Some vfDNA samples were found to contain sufficient amounts of DNA to detect a  
275 chromosomal alteration in a single digital PCR experiment (such as vfDNA-41 in **Figure 5B**).  
276 In other samples, the sensitivity of detecting a CNA was lower, but this could be increased by  
277 repeating the experiment up to three times and merging the results (such as vfDNA-24 in  
278 **Figure 5C**). In general, higher levels of sensitivity were obtained when more droplets could  
279 be analysed, when more melanoma-cell derived vfDNA was present and when less healthy  
280 cell DNA ‘contaminated’ the sample (**Supplementary Table 1**). Moreover, in line with our  
281 earlier observations [19, 20], the SNP-based approach was generally more precise than the  
282 classic alternative (**Figure 5C**) and was chosen as preferred methodology whenever  
283 available.

284  
285 Based on the *in silico* results, we limited further copy number analysis to those vitreous fluid  
286 samples with an expected sensitivity >80% of calling a loss (of chromosome 3p, in 21/39 =  
287 54% of the vfDNA+/UM+ samples) or gain (of chromosome 8q, in 20/39 = 51% of the  
288 vfDNA+/UM+ samples) in the available amount of vfDNA (**Materials and methods and**  
289 **Figure 2**). Within this subgroup, chromosome 3p losses were detected in 13/15 samples with  
290 a known loss in the matched primary tumour. Similarly, chromosome 8q copy number  
291 increases were detected in 15/17 samples with a known chromosome 8q CNA in the tumour.  
292 It is noteworthy that in all four discordant cases, the CNA (that remained undetected in the  
293 vfDNA) was heterogeneously present in the matched primary tumour: two uveal melanomas  
294 had a subclonal loss of chromosome 3p and two a subclonal gain of chromosome 8q  
295 (**Supplementary Table 1**) [20]. We did not detect CNAs in vfDNA+/UM+ samples with no  
296 chromosome 3p (n=6) or 8q (n=3) alterations in the matched primary tumour, nor in a  
297 selection of underpowered vfDNA+/UM+ samples and vfDNA+/UM- samples (which lack  
298 copy number altered melanoma-cell derived DNA). Overall, the presence of chromosome 3p  
299 and 8q alterations matched those in the primary tumour in 19/21 (90%) and 18/20 (90%)  
300 analysable vitreous fluid samples, respectively.

301

302 **Clinicopathological context**

303 Lastly, we investigated whether the vfDNA content correlated to the clinicopathological  
304 context of the primary tumour. First of all, we hypothesised that the detectability of  
305 melanoma-cell derived vfDNA related to anatomical characteristics of the primary tumour  
306 (**Figure 6A and B**). No significant differences were found with regard to the largest basal  
307 diameter and frequency tumours broken through Bruch's membrane, but patients with  
308 melanoma-cell derived vfDNA had a larger prominence of their primary tumour (median 8  
309 versus 6 mm, Mann-Whitney U  $p = 0.018$ ) than those without. Within the vfDNA+/UM+  
310 samples, there was a significant positive correlation between the prominence of primary  
311 tumour and concentration of melanoma-cell derived vfDNA (Spearman's  $\rho = 0.52$ ,  $p <$   
312  $0.001$ , **Figure 6C**).

313  
314 Based on the genetic analysis of the primary tumours [20], the distribution of the various  
315 molecular uveal melanoma subtypes within the vfDNA+/UM- and vfDNA+/UM+ patients was  
316 found to be very similar (**Figure 6D and Supplementary Table 1**). Not unexpectedly, the  
317 absence or presence of melanoma-cell derived vfDNA itself did not show an association with  
318 melanoma-related survival (**Figure 6E**). Focussing on the subsequent vfDNA measurements,  
319 however, the molecular subtype of the primary tumour could be successfully inferred from  
320 27/65 (42%) of the vfDNA samples. Within this subgroup, the prognostic relevance of the  
321 molecular classification was evident (log-rank  $p = 0.020$ , **Figure 6F**): patients with a *BAP1*  
322 mutation and/or monosomy 3p had a median melanoma-related survival of 5.8 years, while  
323 the estimated median survival was not reached in the group of patients with an *EIF1AX*  
324 mutation, *SF3B1* mutation and/or disomy 3p.

## 325 Discussion

326 In various malignancies, the analysis of liquid biopsies has proven to provide clinically-  
327 relevant molecular information of primary or metastatic tumours, while forming a less  
328 invasive alternative to direct tumour biopsies [21, 29]. In ocular oncology, the genetic  
329 analysis of eye fluids has a prominent role in the differentiation between a malignant intra-  
330 ocular lymphoma and a benign uveitis [30], but it remained unexplored in the context of  
331 characterising uveal melanoma. For this reason, we investigated the DNA from the vitreous  
332 fluid as a potential source of molecular information from the primary tumour (**Figure 1**).

333  
334 Firstly, we measured the total amount and fraction of melanoma-cell derived vfdDNA based on  
335 the abundance of mutant and wild-type  $G\alpha_q$  alleles (**Figure 2 and 3**). This analysis was  
336 successful in 97% of the samples, indicating that nearly all vitreous fluids contained  
337 measurable levels of DNA. However, in only 60% of all samples part of this genetic material  
338 was derived from melanoma cells. This indicates that a considerable proportion of the DNA  
339 present in the vitreous originated from non-malignant cells. It would be interesting to further  
340 characterise the cell type of origin of this DNA, for example by applying genetic immune cell  
341 measurements or epigenetic profiling [31-34].

342  
343 Next, we tested the vfdDNA+/UM+ samples for additional DNA alterations. Based on the  
344 known genetic profile of the matched primary tumour, 13/15 (87%) of the analysed vitreous  
345 fluid samples had a measurable BSE mutation (**Figure 2 and 4**). Importantly, however, this  
346 supervised mutational screening is not feasible when no matched tumour material is  
347 available. In such situations, the vfdDNA should be screened for all possible alterations, but  
348 this procedure requires multiple experiments and is sample-expensive. A possible solution  
349 may be found in the development of multiplex setups in which various assays are combined  
350 within one experiment. Our *EIF1AX* drop-off assays furthermore proved that mutation  
351 analyses can be made more generic: all different exon 1 and 2 mutations could be measured  
352 requiring only two distinct assays. Similar drop-off approaches may be developed for the  $G\alpha_q$   
353 signalling mutations and the majority of *SF3B1* mutations. However, it is unlikely that  
354 comparable assays can be developed to generically detect all *BAP1* mutations, as these  
355 mutations do not occur at hotspot positions and are practically unique in each mutant tumour.

356  
357 In addition to the BSE mutations, CNAs were studied in the vfdDNA+/UM+ samples. The  
358 presence of chromosome 3p and 8q alterations corresponded with those in the primary  
359 tumour in 19/21 (90%) and 18/20 (90%) of the analysable cases, respectively (**Figure 2 and**  
360 **5**). Though, we noted that remarkable differences exist in the detectability of melanoma-cell

361 derived mutations versus CNAs: whereas the qualitative identification of any mutant allele  
362 inevitably confirms the presence of this mutation, a CNA can only be detected upon a precise  
363 quantification of the chromosomal target in comparison to the healthy copy number invariant  
364 situation. This leads to sample-specific detection limits that are higher than those for  
365 mutations, especially in samples with large amounts of ‘contaminating’ non-melanoma cell  
366 derived unaltered DNA. In this study, we first evaluated the detectability of CNAs *in silico*,  
367 based on the varying concentrations of (non-)melanoma-cell derived DNA of each individual  
368 sample (**Figure 5**). As a result, roughly half of the vfDNA+/UM+ samples were found to have  
369 a too low total DNA concentration or fraction melanoma-cell derived DNA, and were  
370 technically underpowered to detect chromosomal gains or losses. While this means that no  
371 conclusions can be drawn on the presence of CNAs in these samples, this *in silico* analysis  
372 helped to avoid generating false-negative results and prevented an unnecessary waste of  
373 precious material.

374  
375 Although most of our vfDNA analyses successfully identified the BSE mutation or CNA  
376 present in the primary tumour, a number of cases was discordant (**Figure 2 and**  
377 **Supplementary Table 1**). We noted that the two BSE-lacking vitreous fluid samples  
378 presented extreme low purity ( $< 0.8 G\alpha_q$  mutant copies/uL), which may challenge the  
379 identification of additional mutations with alternative assays. It would be interesting to further  
380 compare all digital PCR mutation assays for their exact lower limits of detection, and to  
381 repeat experiments to exclude vfDNA subsampling and improve the sensitivity of the  
382 mutation detection. In contrast, the four CNA-lacking vitreous fluid samples were predicted to  
383 have sufficient melanoma-cell derived DNA concentrations to detect chromosomal gains and  
384 losses, assuming that the alteration clonally abundant in the entire melanoma-cell derived  
385 fraction vfDNA. Intriguingly, all CNA-discordant cases demonstrated heterogeneity for this  
386 chromosomal loss or gain in the primary tumour. This admixed presence of clones with and  
387 without a certain alteration may explain why it could not be detected in the vitreous fluid: it  
388 may be not present or only present in an undetectable low proportion in the fraction  
389 melanoma-cell derived vfDNA.

390  
391 From a clinical perspective, we found that the detectability of melanoma-cell derived vfDNA  
392 was associated with a higher amount of non-tumour cell derived vfDNA and a larger  
393 prominence of the primary tumour (**Figure 6A and C**). This suggests that larger (and  
394 possibly more invasive) growth of uveal melanomas contributes to the presence of DNA in  
395 the vitreous fluid, originating from both melanoma and other cells. However, the identification  
396 of melanoma-cell derived vfDNA itself did not mark a genetically distinct or prognostically-  
397 relevant subgroup of patients (**Figure 6D and E**). By combining the BSE mutation and CNA

398 results, in 27/65 (42%) of the cases the molecular subtype of the primary tumour could be  
399 successfully inferred from the vfDNA measurements. Within this subgroup, the correlation  
400 between this molecular classification of tumours and patients' risk of developing lethal  
401 metastases was clearly demonstrated (**Figure 6F**).

402  
403 Our findings illustrate that in a proportion of patients, relevant molecular information from  
404 their primary uveal melanoma may be derived from analysing the DNA present in the  
405 vitreous fluid. Following this approach, the risk of metastatic tumour dissemination may be  
406 estimated without a direct tumour biopsy, and an increasing number of patients may be  
407 offered concordant clinical follow-up. Nevertheless, it is crucial to note that in our current  
408 study the vitreous fluid samples were investigated that had been collected ex vivo from  
409 enucleated eyes. This procedure is different to it would be in a clinical setting, and uveal  
410 melanomas treated by enucleation are typically larger and more invasive than irradiated  
411 tumours. Therefore, a follow-up study should evaluate the applicability of our methodology in  
412 a prospective clinical context, for example by defining patient groups most likely to benefit  
413 from the analysis (e.g. those with relatively thick tumours), and by evaluating vfDNA collected  
414 in a similar way as performed in vivo from non-enucleated eyes.

415  
416 One may also consider to explore possible additions and alternatives to our current  
417 methodologies. For example, epigenetic targets (such as DNA methylation) may be  
418 evaluated as markers for the various molecular subtypes of uveal melanomas. Candidate loci  
419 have already been identified [35, 36], and as DNA methylation can be measured using digital  
420 PCR as well [37, 38], the analysis may be easily incorporated in our current workflow.  
421 Additionally, the experimental performance might be optimised to reach lower limits of  
422 detection, for example by denaturing the DNA samples prior to digital PCR analysis [39].  
423 As further alternatives, vitreous fluid samples may be studied using complementary  
424 molecular techniques (such as ultradeep sequencing) or by analysing its RNA, as we  
425 recently showed that tumour-derived genetic information may also be inferred from a  
426 transcriptional level [40].

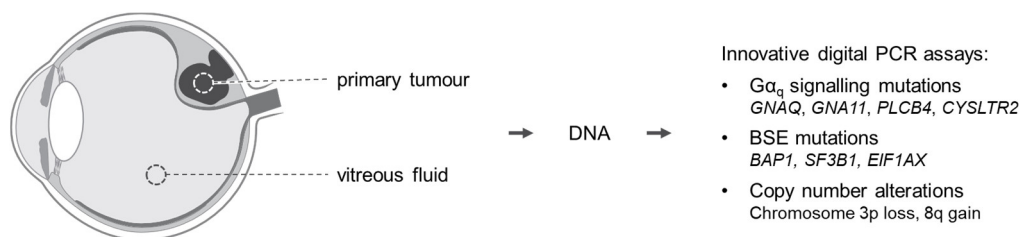
427  
428 Lastly, we believe that our digital PCR assays and approaches have translational potential in  
429 the analysis of heterogeneous solid or liquid uveal melanoma biopsies of any other origin.  
430 Some of the mutation assays described in this study have already been used in blood-based  
431 screening of uveal melanoma patients [41], and the value of similar applications is  
432 increasingly recognised [42].

433

434 In conclusion, our findings demonstrate the possibility of capturing the molecular profile of a  
435 primary uveal melanoma by analysing the DNA present in the vitreous fluid of the eye. As  
436 this approach does not require a biopsy to be taken from the tumour itself, a molecular  
437 classification of the primary tumour and concordant follow-up might be offered to more  
438 patients. In the end, this may ameliorate the clinical outcome of patients with this aggressive  
439 malignancy.

## 440 Figures

### 441 Figure 1



eye with uveal melanoma  
(enucleated, n=65)

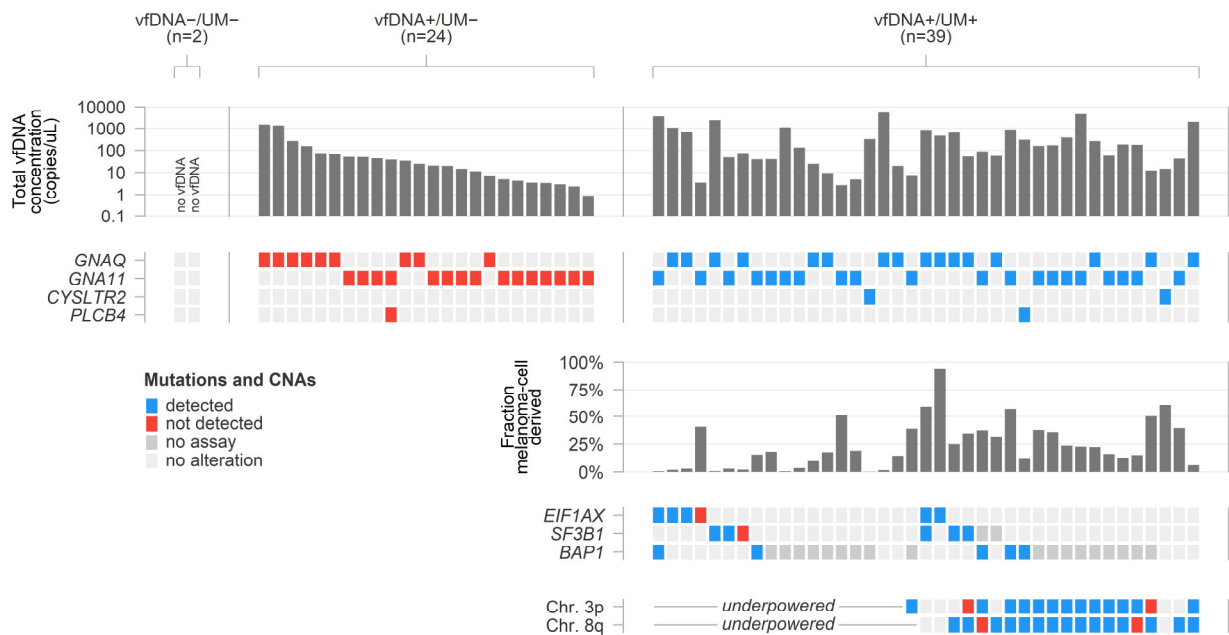
442

443

444 Workflow of current study: DNA from primary tumours [20] and vitreous fluid samples in 65

445 enucleated eyes is analysed by digital PCR.

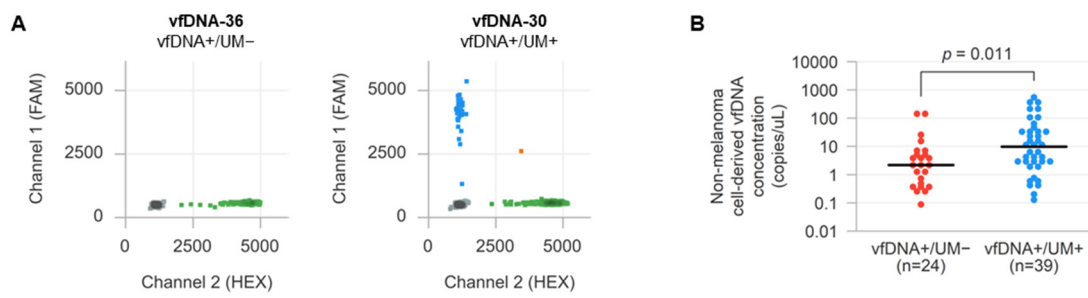
446 **Figure 2**



447

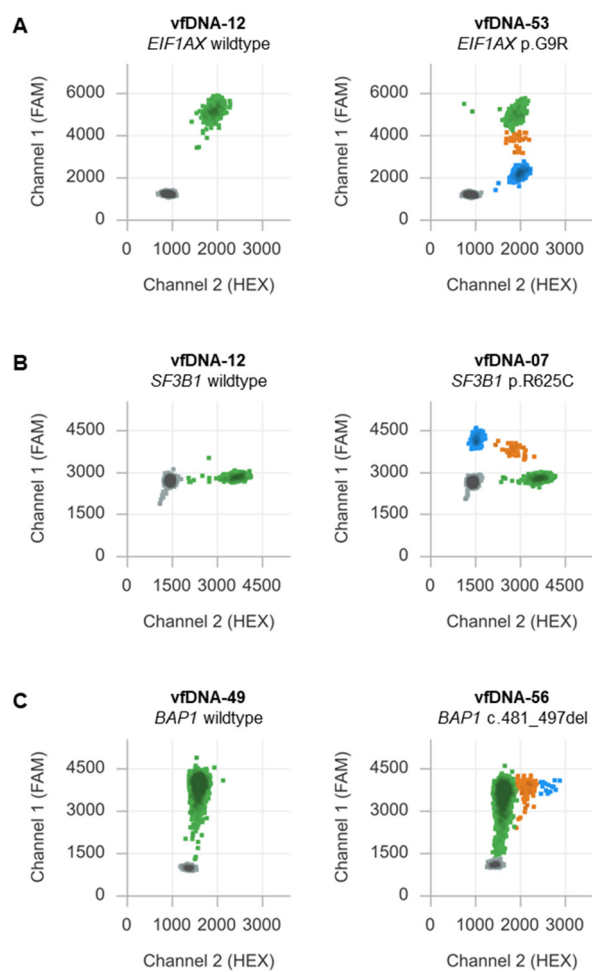
448 DNA composition and detectability of molecular alterations in 65 vitreous fluid samples.  
 449 Mutations and CNAs are compared to those identified in the matched primary tumour [20],  
 450 and their detection in the vfdNA is visualised. 'No assay' refers to a selection of mutations  
 451 that were known to be present in the primary tumour, but could not be analysed in the vfdNA  
 452 sample. 'Underpowered' refers to the condition in which the amount of total and melanoma-  
 453 cell derived vfdNA was predicted to be insufficient to detect chromosomal CNAs.

454 **Figure 3**



455  
456 **(A)** Analysis of  $G\alpha_q$  signalling mutations using targeted digital PCR, here exemplified for the  
457 measurement of *GNA11* p.Q209L mutant and wild-type DNA alleles with two representative  
458 2D plots for a vfDNA+/UM- and vfDNA+/UM+ sample.  
459 **(B)** Comparison of non-melanoma cell-derived DNA concentrations in vfDNA+/UM- and  
460 vfDNA+/UM+ samples.

461 **Figure 4**

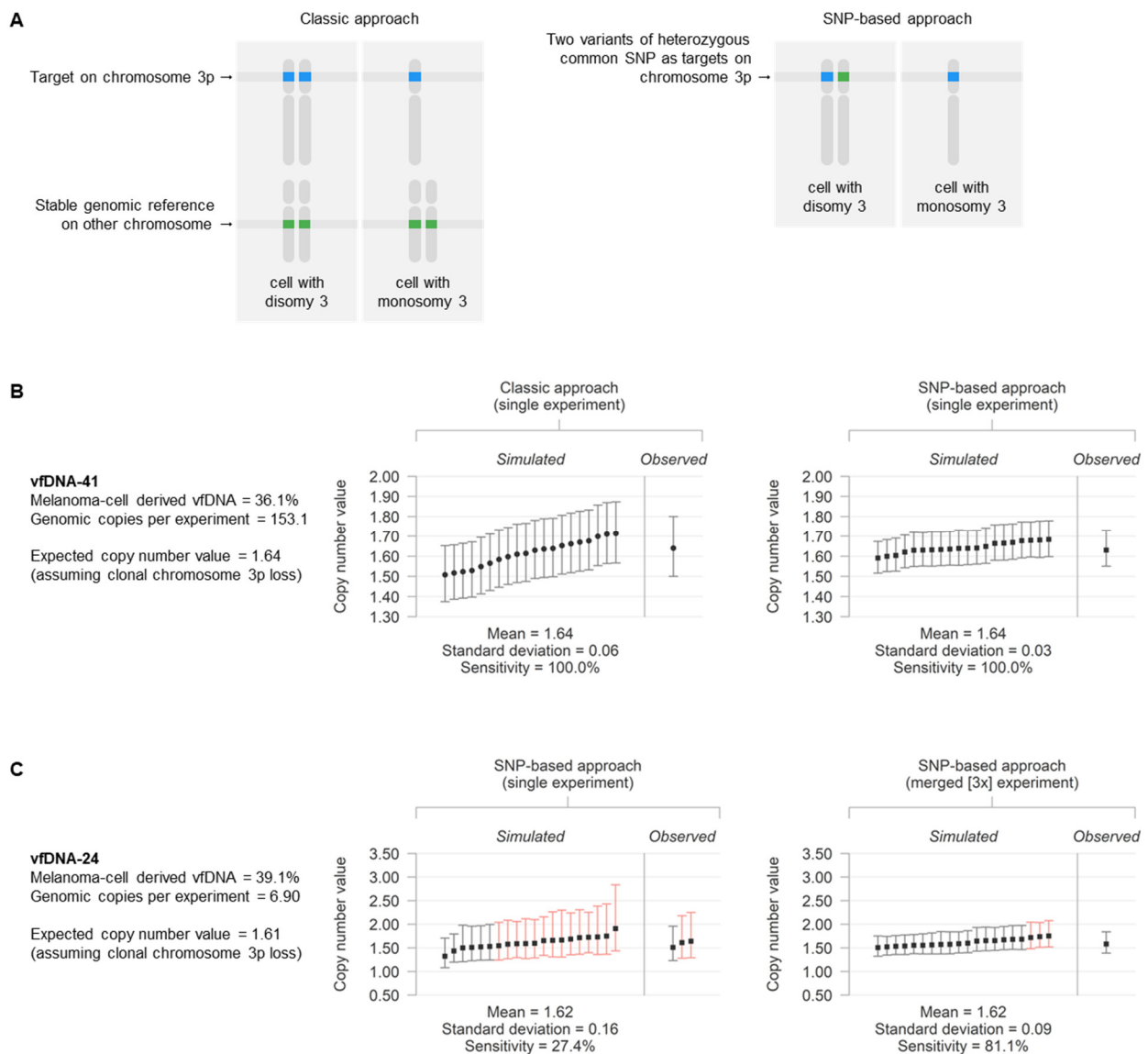


462

463

464 Analysis of BSE mutations in *EIF1AX* (**A**), *SF3B1* (**B**) and *BAP1* (**C**) using drop-off and  
465 targeted digital PCR assays. Here exemplified with the representative 2D plots for a wild-type  
466 and mutant vfDNA sample with similar total vfDNA concentrations.

467 **Figure 5**



468

469

470 **(A)** Approaches to analyse copy number alterations, here exemplified for measuring

471 chromosome 3p loss.

472 **(B)** Simulated and observed copy number value measurements for chromosome 3p in

473 vfDNA-41, with associated confidence intervals. Simulations were based on the initial  $G\alpha_q$

474 mutant and wild-type measurements and the assumption of a clonal loss in the vfDNA

475 melanoma-cell population, in single experiments using both the classic and SNP-based

476 approach. Significance of the measurements is indicated by the colour of the individual

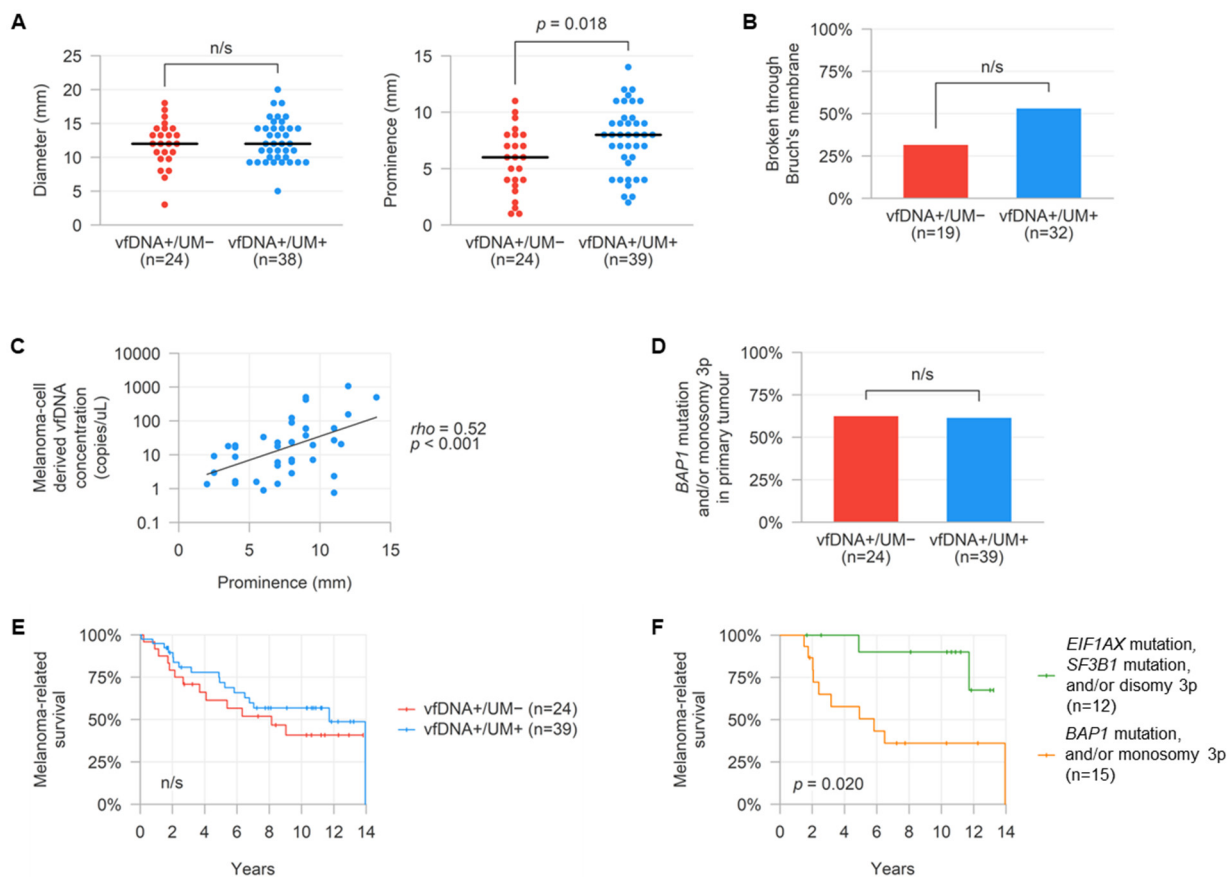
477 confidence interval (red: not significantly different from 2 [ $p > 0.01$ ], grey: significantly

478 different from 2 [ $p < 0.01$ ]).

479 **(C)** Overview of simulated and observed copy number value measurements for chromosome

480 3p in vfDNA-24, in both single and (3x) merged experiments using the SNP-based approach.

481 **Figure 6**



482

483

484 **(A)** Comparison in pathologically-determined largest basal diameter and prominence of  
 485 matched primary tumours in vfdDNA+/UM- or UM+ samples. The black horizontal line  
 486 denotes the median value for both groups.

487 **(B)** Comparison in frequency of pathologically-determined breaching of Bruch's membrane in  
 488 matched primary tumours in vfdDNA+/UM+ and UM- samples.

489 **(C)** Correlation between concentrations of mutant vfdDNA and pathologically-determined  
 490 prominence of matched primary tumours in vfdDNA+/UM+ samples.

491 **(D)** Comparison in frequency of matched primary tumours with a poor prognostic molecular  
 492 subtype (*BAP1* mutation and/or monosomy 3p) in vfdDNA+/UM- or UM+ samples.

493 **(E)** Melanoma-related survival of patients within the vfdDNA+/UM- or UM+ groups.

494 **(F)** Melanoma-related survival of patients based on the inferred molecular subtypes from  
 495 vfdDNA measurements.

## 496 References

- 497 1. Jager, M.J., et al., *Uveal melanoma*. Nat Rev Dis Primers, 2020. **6**(1): p. 24.
- 498 2. Eskelin, S., et al., *Tumor doubling times in metastatic malignant melanoma of the*  
499 *uvea: tumor progression before and after treatment*. Ophthalmology, 2000. **107**(8): p.  
500 1443-9.
- 501 3. Uner, O.E., et al., *Estimation of the timing of BAP1 mutation in uveal melanoma*  
502 *progression*. Sci Rep, 2021. **11**(1): p. 8923.
- 503 4. Martin, M., et al., *Exome sequencing identifies recurrent somatic mutations in EIF1AX*  
504 *and SF3B1 in uveal melanoma with disomy 3*. Nat Genet, 2013. **45**(8): p. 933-6.
- 505 5. Rodrigues, M., et al., *Evolutionary Routes in Metastatic Uveal Melanomas Depend on*  
506 *MBD4 Alterations*. Clin Cancer Res, 2019. **25**(18): p. 5513-5524.
- 507 6. Furney, S.J., et al., *SF3B1 mutations are associated with alternative splicing in uveal*  
508 *melanoma*. Cancer Discov, 2013. **3**(10): p. 1122-1129.
- 509 7. Harbour, J.W., et al., *Recurrent mutations at codon 625 of the splicing factor SF3B1*  
510 *in uveal melanoma*. Nat Genet, 2013. **45**(2): p. 133-5.
- 511 8. Yavuziyigitoglu, S., et al., *Uveal Melanomas with SF3B1 Mutations: A Distinct*  
512 *Subclass Associated with Late-Onset Metastases*. Ophthalmology, 2016. **123**(5): p.  
513 1118-28.
- 514 9. Harbour, J.W., et al., *Frequent mutation of BAP1 in metastasizing uveal melanomas*.  
515 Science, 2010. **330**(6009): p. 1410-3.
- 516 10. Robertson, A.G., et al., *Integrative Analysis Identifies Four Molecular and Clinical*  
517 *Subsets in Uveal Melanoma*. Cancer Cell, 2017. **32**(2): p. 204-220 e15.
- 518 11. Singh, A.D., et al., *Fine-needle aspiration biopsy of uveal melanoma: outcomes and*  
519 *complications*. Br J Ophthalmol, 2016. **100**(4): p. 456-62.
- 520 12. Sellam, A., et al., *Fine Needle Aspiration Biopsy in Uveal Melanoma: Technique,*  
521 *Complications, and Outcomes*. Am J Ophthalmol, 2016. **162**: p. 28-34 e1.
- 522 13. Lieb, M., et al., *Psychosocial impact of prognostic genetic testing in uveal melanoma*  
523 *patients: a controlled prospective clinical observational study*. BMC Psychol, 2020.  
524 **8**(1): p. 8.
- 525 14. Damato, B.E., et al., *Tebentafusp: T Cell Redirection for the Treatment of Metastatic*  
526 *Uveal Melanoma*. Cancers (Basel), 2019. **11**(7).
- 527 15. Bigot, J., et al., *Splicing Patterns in SF3B1-Mutated Uveal Melanoma Generate*  
528 *Shared Immunogenic Tumor-Specific Neopeptides*. Cancer Discov, 2021. **11**(8): p.  
529 1938-1951.
- 530 16. Versluis, M., et al., *Digital PCR validates 8q dosage as prognostic tool in uveal*  
531 *melanoma*. PLoS One, 2015. **10**(3): p. e0116371.
- 532 17. de Lange, M.J., et al., *Heterogeneity revealed by integrated genomic analysis*  
533 *uncovers a molecular switch in malignant uveal melanoma*. Oncotarget, 2015. **6**(35):  
534 p. 37824-35.
- 535 18. Nell, R.J., et al., *Involvement of mutant and wild-type CYSLTR2 in the development*  
536 *and progression of uveal nevi and melanoma*. BMC Cancer, 2021. **21**(1): p. 164.
- 537 19. Nell, R.J., et al., *Allele-specific digital PCR enhances precision and sensitivity in the*  
538 *detection and quantification of copy number alterations in heterogeneous DNA*  
539 *samples: an in silico and in vitro validation study*. medRxiv, 2023.
- 540 20. Nell, R.J., et al., *Digital PCR-based deep quantitative profiling delineates*  
541 *heterogeneity and evolution of uveal melanoma*. medRxiv, 2024.
- 542 21. Olmedillas-Lopez, S., M. Garcia-Arranz, and D. Garcia-Olmo, *Current and Emerging*  
543 *Applications of Droplet Digital PCR in Oncology*. Mol Diagn Ther, 2017. **21**(5): p. 493-  
544 510.
- 545 22. Zoutman, W.H., R.J. Nell, and P.A. van der Velden, *Usage of Droplet Digital PCR*  
546 *(ddPCR) Assays for T Cell Quantification in Cancer*. Methods Mol Biol, 2019. **1884**: p.  
547 1-14.

- 548 23. Van Raamsdonk, C.D., et al., *Frequent somatic mutations of GNAQ in uveal*  
549 *melanoma and blue naevi*. *Nature*, 2009. **457**(7229): p. 599-602.
- 550 24. Van Raamsdonk, C.D., et al., *Mutations in GNA11 in uveal melanoma*. *N Engl J Med*,  
551 2010. **363**(23): p. 2191-9.
- 552 25. Johansson, P., et al., *Deep sequencing of uveal melanoma identifies a recurrent*  
553 *mutation in PLCB4*. *Oncotarget*, 2016. **7**(4): p. 4624-31.
- 554 26. Moore, A.R., et al., *Recurrent activating mutations of G-protein-coupled receptor*  
555 *CYSLTR2 in uveal melanoma*. *Nat Genet*, 2016. **48**(6): p. 675-80.
- 556 27. Vader, M.J.C., et al., *GNAQ and GNA11 mutations and downstream YAP activation*  
557 *in choroidal nevi*. *Br J Cancer*, 2017. **117**(6): p. 884-887.
- 558 28. Durante, M.A., et al., *Genomic evolution of uveal melanoma arising in ocular*  
559 *melanocytosis*. *Cold Spring Harb Mol Case Stud*, 2019. **5**(4).
- 560 29. Lone, S.N., et al., *Liquid biopsy: a step closer to transform diagnosis, prognosis and*  
561 *future of cancer treatments*. *Mol Cancer*, 2022. **21**(1): p. 79.
- 562 30. de Hoog, J., et al., *Combined cellular and soluble mediator analysis for improved*  
563 *diagnosis of vitreoretinal lymphoma*. *Acta Ophthalmol*, 2019. **97**(6): p. 626-632.
- 564 31. Zoutman, W.H., et al., *Accurate Quantification of T Cells by Measuring Loss of*  
565 *Germline T-Cell Receptor Loci with Generic Single Duplex Droplet Digital PCR*  
566 *Assays*. *J Mol Diagn*, 2017. **19**(2): p. 236-243.
- 567 32. de Lange, M.J., et al., *Digital PCR-Based T-cell Quantification-Assisted*  
568 *Deconvolution of the Microenvironment Reveals that Activated Macrophages Drive*  
569 *Tumor Inflammation in Uveal Melanoma*. *Mol Cancer Res*, 2018. **16**(12): p. 1902-  
570 1911.
- 571 33. Zoutman, W.H., et al., *A novel digital PCR-based method to quantify (switched) B*  
572 *cells reveals the extent of allelic involvement in different recombination processes in*  
573 *the IGH locus*. *Mol Immunol*, 2022. **145**: p. 109-123.
- 574 34. van de Leemkolk, F.E.M., et al., *Quantification of Unmethylated Insulin DNA Using*  
575 *Methylation Sensitive Restriction Enzyme Digital Polymerase Chain Reaction*.  
576 *Transpl Int*, 2022. **35**: p. 10167.
- 577 35. Field, M.G., et al., *BAP1 Loss Is Associated with DNA Methyloomic Repatterning in*  
578 *Highly Aggressive Class 2 Uveal Melanomas*. *Clin Cancer Res*, 2019. **25**(18): p.  
579 5663-5673.
- 580 36. Bakhoun, M.F., et al., *BAP1 methylation: a prognostic marker of uveal melanoma*  
581 *metastasis*. *NPJ Precis Oncol*, 2021. **5**(1): p. 89.
- 582 37. Nell, R.J., et al., *Quantification of DNA methylation independent of sodium bisulfite*  
583 *conversion using methylation-sensitive restriction enzymes and digital PCR*. *Hum*  
584 *Mutat*, 2020. **41**(12): p. 2205-2216.
- 585 38. Salgado, C., et al., *Interplay between TERT promoter mutations and methylation*  
586 *culminates in chromatin accessibility and TERT expression*. *PLoS One*, 2020. **15**(4):  
587 p. e0231418.
- 588 39. Fitarelli-Kiehl, M., et al., *Denaturation-Enhanced Droplet Digital PCR for Liquid*  
589 *Biopsies*. *Clin Chem*, 2018. **64**(12): p. 1762-1771.
- 590 40. Nell, R.J., et al., *Identification of clinically-relevant genetic alterations in uveal*  
591 *melanoma using RNA sequencing*. *medRxiv*, 2023.
- 592 41. Beasley, A., et al., *Clinical Application of Circulating Tumor Cells and Circulating*  
593 *Tumor DNA in Uveal Melanoma*. *JCO Precis Oncol*, 2018. **2**.
- 594 42. Carvajal, R.D., et al., *Clinical and molecular response to tebentafusp in previously*  
595 *treated patients with metastatic uveal melanoma: a phase 2 trial*. *Nat Med*, 2022.  
596 **28**(11): p. 2364-2373.  
597

598 **Supplementary information**

599 **Supplementary Table 1**

600 Overview of clinical and molecular information of all cases analysed in this study.